Magnetic Properties of High-Pressure Torsion Deformed Co-zr

Martin Stückler , Stefan Wurster , Markus Alfreider , Michael Zawodzki , Heinz Krenn , Andrea Bachmaier *

Posted Date: 10 July 2023

doi: 10.20944/preprints202307.0635.v1

Keywords: severe plastic deformation; amorphous alloys; magnetic properties; nanocrystallization

Article

Magnetic Properties of High-Pressure Torsion Deformed Co-Zr

Martin Stückler [a], Stefan Wurster [a], Markus Alfreider [b], Michael Zawodzki [a], Heinz Krenn [c] and Andrea Bachmaier [a,*]

[a] Erich Schmid Institute of Materials Science of the Austrian Academy of Sciences, 8700 Leoben, Austria; martin.stueckler@gmail.com (M.S.), stefan.wurster@oeaw.ac.at (S.W), michael.zawodzki@oeaw.ac.at (M.Z.), andrea.bachmaier@oeaw.ac.at (A.B)

[b] Department Materials Science, Montanuniversität Leoben, 8700 Leoben, Austria; markus.alfreider@unileoben.ac.at (M.A.)

[c] Institute of Physics, University of Graz, 8010 Graz, Austria; heinz.krenn@uni-graz.ac.at (H.K.)

* Correspondence: author: Andrea Bachmaier

Abstract: Co-Zr amorphous alloys exhibit soft magnetic properties, whereas Co-rich crystalline magnetic phases in this alloy system display hard magnetic behaviour. In this study, an initial two-phase Co-Zr composite with an overall composition of 75 at.% Co and 25 at.% Zr was processed by high pressure torsion (HPT) and the effects of severe plastic deformation and subsequent thermal treatment on the structural evolution and its magnetic properties have been investigated. HPT processing allowed us to achieve an amorphous microstructure in the as-deformed state with low coercivity. To further tune magnetic properties and study the alloys' crystallization behaviour, various annealed states are investigated. Microstructural properties are correlated to the magnetic properties and a decreasing coercivity with increasing annealing temperature is observed despite the onset of crystallization in the amorphous alloy. At higher annealing temperatures, coercivity increases again. The results appear promising to obtain tuneable rare-earth free magnetic materials by severe plastic deformation.

Keywords: severe plastic deformation; amorphous alloys; magnetic properties; nanocrystallization

1. Introduction

The use of severe plastic deformation by high-pressure torsion (HPT) deformation for production of bulk magnetic materials has been demonstrated in several studies and reviews summarizing the results have been recently published [1,2]. For example, HPT deformed SmCo-Fe composites have been investigated regarding their hard magnetic properties [3,4]. Regarding soft magnetic materials, HPT deformed supersaturated Co-Cu solid solutions provide tunability in the magnetic moment and the coercivity by varying the Co-to-Cu ratio [5,6]. Soft magnetic properties have been observed for high Co-contents [5] and a further improvement was achieved by substituting small amounts of Co with Fe [7]. Some commercial soft magnetic materials consist of an amorphous matrix, in which a crystalline, ferromagnetic phase is embedded [8]. Thus, further improvements in terms of soft magnetic properties is expected by formation of a similar microstructure by HPT. To achieve this goal, combinations of elements have to be used, which enable the formation of an amorphous structure. During mechanical alloying, the formation of amorphous microstructures in a large variety of systems, for example using combinations of transition metals with Zr and Ti, have been already observed [9–13]. Amorphization during HPT deformation has also been reported for certain material combinations and compositions [14].

In this study, HPT induced amorphization in the Co-Zr system and its magnetic properties in as-deformed and annealed states is investigated. In the 80 and 90s, a lot of research was conducted on Co-Zr amorphous soft magnetic materials due to its low coercive force, high permeability and high saturation magnetization, for example to be used in read heads for magnetic recording [15]. Shimada and Kojima demonstrated that annealing of Co-Zr amorphous thin films has a strong

positive effect on coercivity [16]. Depending on the composition (5-17at. % Zr), soft magnetic properties (Hc < 1Oe) were achieved in a temperature range between 300°C - 500°C [16]. A high saturation magnetization in combination with a relatively low magnetostriction was also reported. Naoe et al. [17] showed that the saturation magnetization decreases with increasing Zr-content. A high saturation magnetization was achieved if the Zr content was as low as 2 at. %. Amorphization of Co-Zr during ball milling has been reported to be successful for composition of 27-92at.% Co [11,18]. Furthermore, it is important to note that different Co-Zr phases with lower Zr Content exhibit hard magnetic behaviour [19].

The overall composition of the HPT deformed samples in this study is 75 at. % Co and 25 at. % Zr. On the one hand, this composition is chosen because it lies right within the window of amorphization via ball milling and being close to the transition metal - Zr composition, where amorphization was already induced via HPT deformation for applied equivalent shear strains above ε=400 [14]. On the other hand, the composition is close to the cubic Laves phase compound $ZrCo_2$ [20]. It has been shown that $ZrCo_2$ can accommodate excess Co up to the composition $ZrCo_3$ and the magnetic properties strongly depend on the amount of excess Co. $ZrCo_2$ is strongly paramagnetic at RT. Ferromagnetism is observed in $ZrCo_x$ for $2.8 \leqslant x \leqslant 3.0$. [21,22]. To achieve soft magnetic properties in the severely deformed material, the idea is to induce an amorphous microstructure by HPT, in which a ferromagnetic phase is embedded by subsequent annealing at low temperatures. This ferromagnetic phase might be either the aforementioned Co rich $ZrCo_x$ phase or the other hard magnetic phases with compositions at slightly lower Zr contents. Further tuning of the magnetic properties might be possible by prolonged annealing or by applying higher annealing temperatures for short times.

For processing the Co-Zr composite material, the HPT-multi-sector disc method was used [23]. This method combines the advantage of HPT deformation of bulk-samples (no powder processing, less oxidation and less impurities due to lower amount of free surfaces, no complicated storage and handling in inert gas atmosphere which is even more crucial for Zr-powders) with the one of powder-HPT (no need of pre-processing the material - ball milling or arc-melting for „mixing“ the desired material). Simultaneously, the advantage to process any desired material composition is maintained.

2. Material and methods

The following initial materials were used for sample processing: bulk Co - purity 99.95%, MaTeck; bulk Zr (Zr 702, from ATI, min. Zr content of 99.2wt% with Hf being the main alloying element (max. 4.5%). For the multi-sector disc method, 6 bulk segments in total were produced by electro discharge machining. The central angle for each of the 3 Zr-pieces and 3 Co-pieces was 50° and 70° respectively. Taking into account the nominal mass density, the overall composition corresponds to Co_3Zr. The actual HPT-sample was then composed of these individual sectors made from the two different materials and alternatingly stacked together to build the actual disk with a diameter of 30 mm and a thickness of 6.35 mm before HPT processing. HPT deformation was performed at room temperature using a nominal pressure of 5 GPa. Due to discontinuous outflow of material from the anvil cavities during the deformation process, anvils came into contact and the HPT deformation had to be stopped. To increase the amount of applied strain, a reworking of anvils, lowering their cavity depth, was performed twice. This results in a reduction of the initial sample height from 6.35 mm to 4.00 mm, 3.50 mm and 2.00 mm after the first, second and third HPT-processing step, respectively. The applied equivalent strains for each processing step were summed up, resulting in a maximum applied strain of ε~1100 for r=15 mm after the last HPT processing step.

Vickers hardness measurements were made in axial direction, using a microindentation hardness tester from Buehler (Micromet 5104) using a load of 1000gf. Indents were made along the radius at a distance of 0.25 mm in axial direction. X-ray diffraction (XRD) measurements of the as-deformed state were initially done with a Phaser Bruker D2 diffractometer. Chemical composition was confirmed using an energy dispersive X-ray spectroscope (EDX, e-flash, Bruker) attached to a scanning electron microscope (Tescan Magna).

 doi:10.20944/preprints202307.0635.v1

To conduct annealing treatments, HPT deformed samples were annealed at different temperatures and times (300°C, 400°C, 500°C, 600°C for 1h) in a conventional furnace. An additional sample was annealed at 600°C for 100h in a vacuum furnace.

DC-hysteresis measurements were performed using a superconducting quantum interference device (SQUID, Quantum Design MPMS-XL-7) at 300 K in magnetic fields up to 7 T. The results of the hysteresis measurements were corrected using a Pd-standard, yielding more accurate results for the coercivity H. Saturation magnetization was determined by extrapolating at high fields the mass magnetization as a function of 1/H to zero. For chosen specimens, zero-field-cooling/field-cooling (ZFC-FC) measurements were recorded between 5 K and 300 K at 5 mT.

The deformed and annealed samples were further investigated using high energy XRD in transmission with a beam energy of 87.1 keV (112.5keV for 100h annealed sample) at Deutsches Elektronen-Synchrotron DESY, Hamburg, Germany. To study the microstructure of the at 300°C and 600°C for 1h annealed sample, transmission electron microscopy (TEM)-investigations (JEOL 2200-FS) were further conducted.

3. Results and discussion

The chemical composition of the sample was determined using EDX to be (76.5 +/- 1.6) at% Co and (23.5 +/- 1.6) at% Zr. In Figure 1, the hardness as a function of equivalent strain is plotted for the as-deformed sample after the three step deformation process. Due to the three-step HPT-process, the equivalent strain can only be considered as an estimate. For a radius < 6 mm, which corresponds to an equivalent strain below ε~425, a rather constant microhardness with a mean value of 392+/-21 HV is measured. For higher applied strains (i.e. increasing sample radius), a steady increase in hardness is visible. At the outer edge of the HPT sample, the hardness reaches values of about 600 HV, which is significantly higher compared to the hardness in the inner plateau region. As it is described in Sun et al. for Cu-Zr [14], there is a certain applied strain necessary for the formation of amorphous material during HPT processing. Therein, it was formulated that this critical strain is reached at an equivalent strain of about 400 for Cu29at%Zr. Comparing the hardness values in Figure 1, an increase in hardness at about the same strain is visible and is attributed to the gradual formation of an amorphous phase during HPT processing. XRD measurements at a position with r > 14 mm, show - within the detection limits of the XRD equipment - a fully amorphous material with the composition Co_3Zr (inset in Figure 1). Thus, it can be concluded that for $Co_{75}Zr_{25}$ HPT induced amorphization starts at an equivalent strain of about 400, which leads to a remarkable increase of hardness and to a final hardness of about 600 HV. In amorphous thin films with a slightly lower Zr content, a Vickers hardness of 600 is reported as well [24].

Preprints (www.preprints.org) | NOT PEER-REVIEWED | Posted: 10 July 2023 doi:10.20944/preprints202307.0635.v1

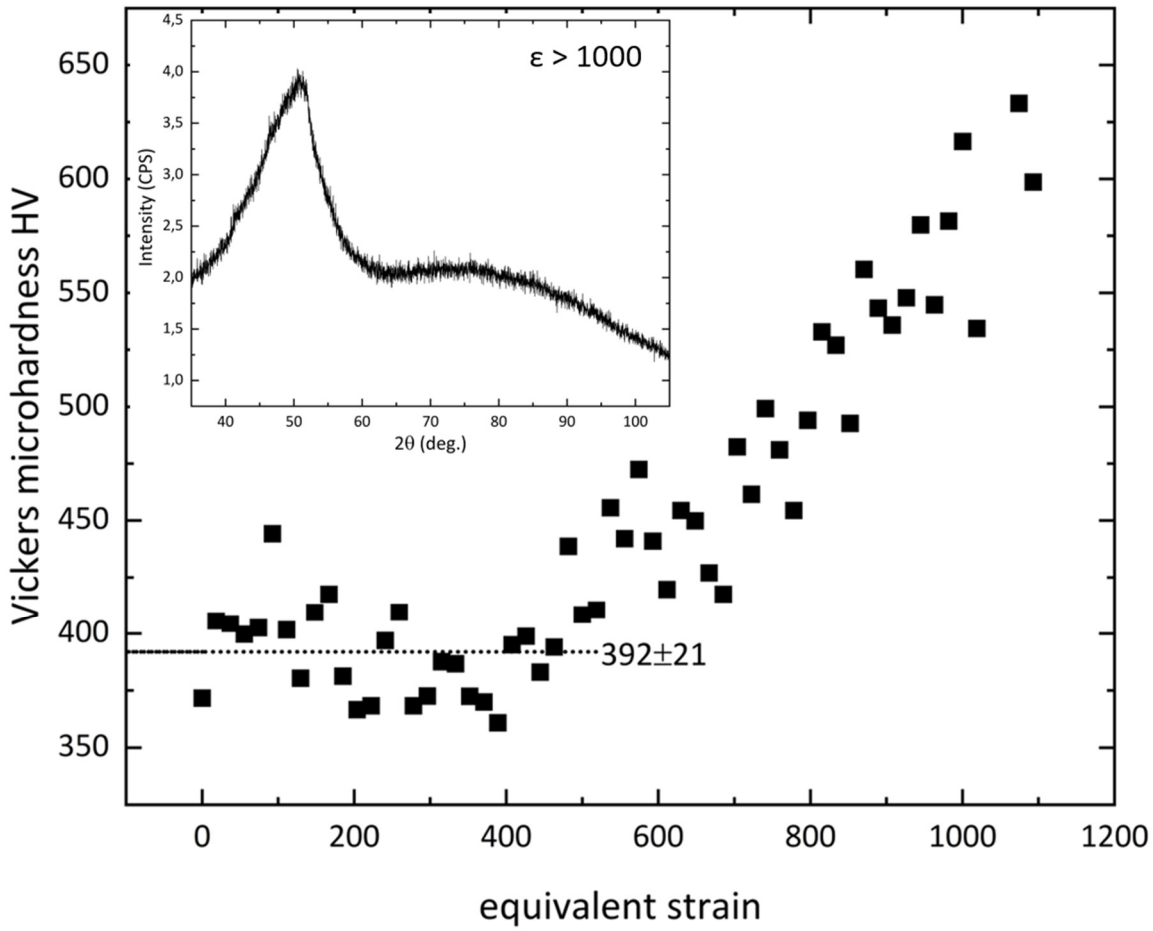

Figure 1. Vickers hardness as a function of equivalent strain. The inset shows the XRD pattern from HPT deformed Co-Zr sample taken from a radius r > 14 mm (according to a strain of ε > 1000).

For the as deformed Co-Zr sample, which consists of amorphous Co-Zr, a coercivity of 6.3 kA/m and a mass magnetization of 49.1 Am^2kg^{-1} was measured. Amorphous Co-Zr is reported to be a moderately strong ferromagnet, which is magnetically soft with a high saturation magnetization [16,17,24,25]. Shimada and Kojima [16] found for $Co_{87}Zr_{13}$ samples a tremendous decrease in coercive force after annealing the sputtered film at 350°C for 30 min. Fe-based nanocrystalline alloys obtained through isothermal annealing of their amorphous counterparts further exhibit excellent soft magnetic materials [26]. Thus, annealing treatments after HPT processing of Co-Zr are conducted in this study to generate a microstructure, which has improved soft magnetic properties. HPT deformed samples were first annealed at different temperatures (300°C, 400°C, 500°C, 600°C) for 1h each. Results of SQUID DC-hysteresis measurements of the as-deformed and annealed samples are shown in Figure 2. Saturation magnetization constantly decreases with increasing annealing temperature, indicating the formation of non-magnetic phases. The coercivity, derived from the hysteresis after correcting for a Pd-standard, drops from 6.3 kA/m to 4.6-4.8 kA/m for intermediate annealing temperatures while it increases again to more than 7.4 kA/m for the highest annealing temperature of 600°C. The drop at intermediate temperatures might be attributable to a relaxation of the amorphous material at temperatures smaller than 300°C, in particular a reduction in residual stresses upon slight annealing. It is known, that HPT-processed samples exhibit a high amount of residual stresses in the as-deformed state [27,28]. From a quick glance, the general trend is in accordance with the results on amorphous and annealed FeCuNbSiB [26], where upon initial crystallization out of the amorphous matrix, coercivity decreases. At higher annealing temperatures, coercivity increases again

Preprints (www.preprints.org) | NOT PEER-REVIEWED | Posted: 10 July 2023 doi:10.20944/preprints202307.0635.v1

with increasing grain size in the FeCuNbSiB alloy. However, in this study the complex CoZr phase diagram [20] and the contribution of different evolving phases also has to be taken into account.

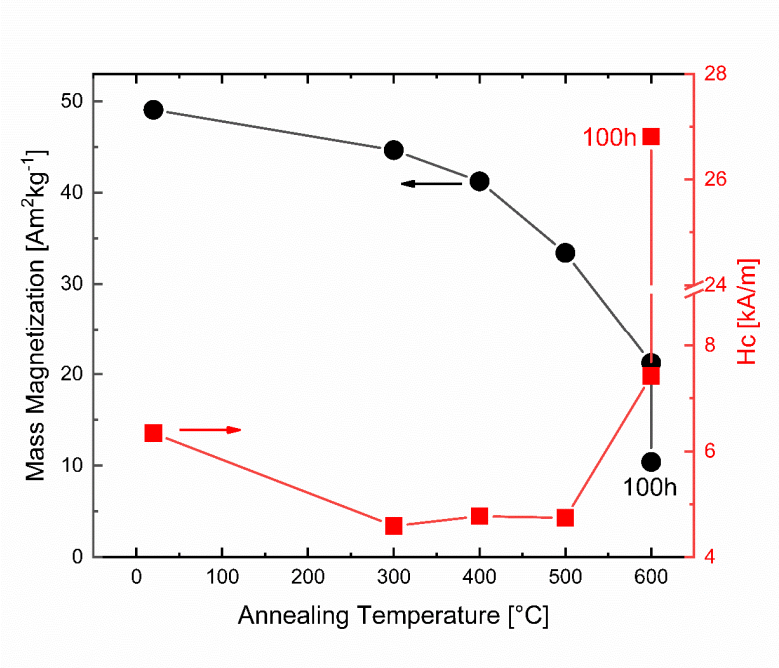

Figure 2. Mass magnetization and coercivity for the as-deformed state and as a function of annealing temperature (300°C, 400°C, 500°C, 600°C for 1h and 100h; ε > 1000 for all samples). The saturation magnetization of pure hcp Co is 162 Am^2kg^{-1} [29].

For detailed phase determination, as-deformed and annealed samples were investigated using high energy XRD (Figure 3). The high energy XRD-data was evaluated using profile analysis of selected area diffraction (PASAD) software obtained via integration over all azimuthal angles [30]. The high energy XRD results confirm the broad peak from the amorphous phase in the as-deformed state (ε > 1000). At the lowest annealing temperature (300°C), the amorphous phase prevails as is confirmed by TEM investigations (not shown). Broad peaks from the amorphous phase remain visible even up to the highest annealing temperature of 600°C. Additionally, small, broad peaks at positions fitting to the cubic CoZr phase (a=3.181Å [31]) appear after annealing at 400°C and 500°C. In the cubic, paramagnetic CoZr structure, Co atoms are surrounded by non-magnetic Zr, thus losing its ferromagnetic character [32]. For the sample annealed at 600°C, additional peaks at different positions appear, whereas the peaks of the cubic CoZr phase vanish. There is a better agreement of the peak positions with the Co_2Zr phase ($MgCu_2$ type), although the peak positions are slightly shifted to smaller lattice spacing. From least square fitting, a smaller lattice spacing of 6.893 Å is derived. Fujii [22] also found a decrease in lattice spacing with increasing Co-content of Co_xZr from ~6.95A for X=2 to ~6.86A for X=3. In Figure 3, these modified peak positions ($Co_{2.6}Zr$) are indicated as well. Fuji et al. [22] describe Co_xZr being ferromagnetic for $2.8 < x < 3$. Combining their data with the one of Aoki et al. [33] they suspected an increasing ferromagnetic moment right at the composition $Co_{2.6}Zr$; thus the $Co_{2.6}Zr$ phase in the annealed sample might be right at the transition from paramagnetic to weakly ferromagnetic state. For Co_3Zr and $Co_{2.8}Zr$, the two ferromagnetic, crystalline phases investigated by Fuji et al. [22], Curie temperatures below 200 K were found. Another hint for the existence of a non-magnetic $Co_{2.6}Zr$ phase after HPT deformation and annealing is an additional FC-measurement (not shown) starting from 400K. It was found that the moment increases linearly with decreasing temperature, giving no indication for a Curie temperature below 400K. In addition, peaks of the magnetic $Co_{23}Zr_6$ phase are found after annealing at 600°C for 1h. The amorphous phase nearly vanished after annealing at 600°C for 1h, which is further confirmed by TEM investigations, which shows a nanocrystalline microstructure (Figure 4).

Preprints (www.preprints.org) | NOT PEER-REVIEWED | Posted: 10 July 2023 doi:10.20944/preprints202307.0635.v1

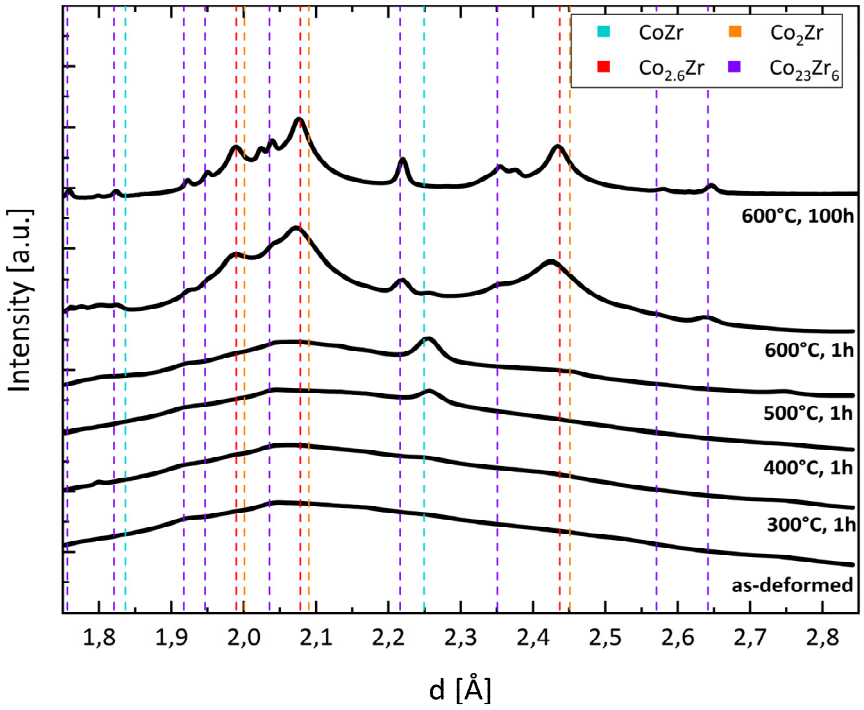

Figure 3: High energy XRD diffractograms for as-deformed and annealed samples ($\varepsilon > 1000$). The peak positions for CoZr, Co_2Zr and $Co_{23}Zr_6$ are indicated. In addition, the peak position of a modified Co_2Zr-phase (red vertical line) with a higher Co-content ($Co_{2.6}Zr$) is indicated.

To further tune the magnetic properties and achieve a complete crystalline microstructure, prolonged annealing at the highest annealing temperature was performed. In Figure 3, the diffractogram of the sample annealed for 100h at 600°C in vacuum is also shown. In this case, the same phases ($Co_{2.6}Zr$ and $Co_{23}Zr_6$) as after annealing at 600°C for 1h are detected, but the amorphous phase vanishes completely. Few peaks in the diffractogram remain, however, unidentified. The peak positions of these peaks do not fit to hcp and fcc Co or pure Zr. They further do not match to various oxides or other magnetic Co-Zr phases with lower Zr content ($ZrCo_{5.1}$ and Zr_2Co_{11}), which might form during the annealing treatment. For the 600°C for 100h annealed Co-Zr sample, which consists of crystalline $Co_{2.6}Zr$ and $Co_{23}Zr_6$ phases, coercivity increases to 26.8 kA/m, and but saturation magnetization decreases to 10.4 Am^2kg^{-1} (Figure 2).

 doi:10.20944/preprints202307.0635.v1

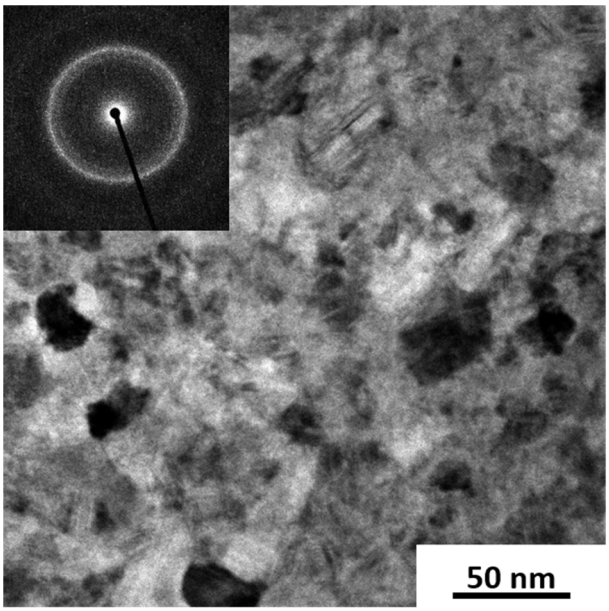

Figure 4. Bright field and selected area electron diffraction image of the at 600°C for 1h annealed sample.

Additionally, the temperature dependence of the low-field susceptibility was investigated for selected annealed samples (300°C, 500°C and 600°C for 1h), which are shown in Figure 5. For ZFC measurements the demagnetized sample is cooled in zero applied field, whereas at the lowest temperature an external field of 5 mT is applied and the magnetic moment is recorded during heating. In FC temperature scans, the magnetic moment is measured during cooling in the same external field. The 300°C and 500°C annealed samples show no splitting between the ZFC/FC-scans displaying a reversible ferromagnetic behaviour. The sample annealed at 600°C exhibits a splitting and a broad peak in the ZFC-FC curve, which is a typical behaviours for thermal activation and a broad ferromagnetic particle distribution in a non-magnetic matrix [34,35]. The increase in coercivity for the 600°C annealed material is due to the ferromagnetic long-range order between the $Co_{23}Zr_6$ phase in the non-magnetic $Co_{2.6}Zr$ phase.

Preprints (www.preprints.org) | NOT PEER-REVIEWED | Posted: 10 July 2023 doi:10.20944/preprints202307.0635.v1

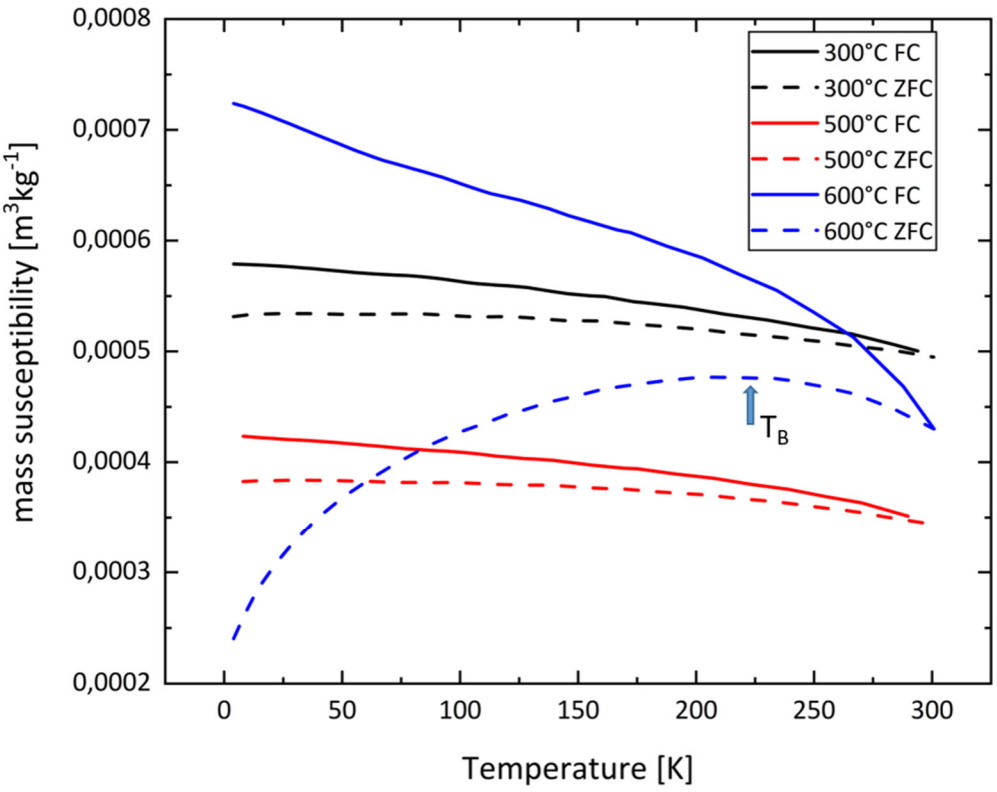

Figure 5. ZFC and FC curves of annealed samples. In all measurements a field of H = 5 mT is applied. Solid lines represent FC-curves, dashed lines represent ZFC-curves. The broad hump at T_B is reminiscent of a "blocking" of non-relaxed ferromagnetic entities ($Co_{23}Zr_6$) in a non-magnetic (or weak paramagnetic) $Co_{2.6}Zr$ matrix.

In summary, the amorphous microstructure possesses a semi-hard magnetic behaviour. After annealing, soft magnetic properties are improved while mostly maintaining the amorphous state. First crystalline diffraction peaks observed at 500°C correspond to the non-magnetic Co-Zr phase, whereas the peaks observed on completion of the crystallization process belong to $Co_{23}Zr_6$ forming small particles with a broad size distribution giving rise to the measurable mass magnetization and a hyper-stoichiometric Co_2Zr phase, most likely $Co_{2.6}Zr$ still being paramagnetic. For our longest annealing time of 100h at 600°C, the peaks become more pronounced and we find again, according to the phase diagram [20], the $Co_{23}Zr_6$ phase and the Co-enriched Co_2Zr phase.

The amorphous phase in deposited CoZr alloys can be stabilized with a small amount of Zr. Typically, 5-6 at.% Zr is sufficient for achieving a uniformly amorphous structure with room temperature deposition [16,17]. Future work will thus consider synthesizing amorphous samples with higher Co content by HPT deformation followed by optimized annealing treatments. On the one hand to achieve better soft magnetic properties due to the increased Co content, on the other hand to obtain other crystallization products like the promising rare-earth free Zr_2Co_{11} phase [36,37] by suppressing the formation of $Co_{23}Zr_6$.

4. Conclusion

Amorphous CoZr alloys are known for their excellent soft-magnetic behaviour, but also hard magnetic phases are found in this alloy system. Therefore, this paper considered the potential of SPD to synthesize bulk amounts of amorphous Co-Zr magnetic material with a simple processing scheme.

Using the HPT multi-sector disc method, material with the overall composition of Co_3Zr was processed. A crystalline-amorphous transition is found at high applied shear strains. The amorphous state is confirmed by high energy XRD measurements. Annealing treatments at temperatures up to 600°C for 1h were performed for relaxing the as-deformed state on the first hand and to induce the growth of nanocrystalline, magnetic phases. SQUID-magnetometry reveals a semi-hard magnetic behaviour for the amorphous state with annealing at moderate temperatures having a beneficial effect on coercivity, where a drop of ~25% compared to the as-deformed state was measured. However, saturation magnetization decreased. Annealing at higher temperatures leads to crystallization and a nanocrystalline microstructure for the highest annealing temperature. Coercivity increases with the formation of the magnetic $Co_{23}Zr_6$ out of the intermediately formed CoZr-phase. The microstructure change, however, also had an impact on the saturation magnetization. The saturation magnetization for the samples receiving the 1h thermal treatment decreased with increasing temperature The further decrease in saturation magnetization after 100h annealing at 600°C can be attributed to ongoing formation of paramagnetic Co_2Zr phase, whose chemical composition was found to be $Co_{2.6}Zr$. This work provides a new approach for further development of HPT processed Co-Zr magnetic materials with higher Co-content and optimized thermal treatments, as they are expected to show even better magnetic properties.

Author Contributions: Conceptualization, M.S. and A.B.; Methodology, all.; Validation, all; Formal Analysis, M.S, S.W. and A.B.; Investigation, M.S., M.Z., M.A..; Resources, H.K.; Data Curation, M.S. and A.B..; Writing – Original Draft Preparation, M.S., S.W. and A.B.; Writing – Review & Editing, all.; Visualization, M.S, M.A. and A.B.; Supervision, A.B.; Project Administration, A.B.; Funding Acquisition, A.B.

Funding: This project has received funding from the European Research Council (ERC) under the European Union's Horizon 2020 research and innovation programme (Grant No. 757333).

Data availability: Data will be made available on request.

Acknowledgments: We acknowledge DESY (Hamburg, Germany), a member of the Helmholtz Association HZ Hereon, for the provision of experimental facilities.

Conflicts of Interest: The authors declare no conflict of interest.

References

1. Z.-R. Wang: P.-Z. Si, J. Park, C.-J. Choi, H.-L. Ge, A Review of Ultrafine-Grained Magnetic Materials Prepared by Using High-Pressure Torsion Method, Materials (Basel). 15 (2022). doi:10.3390/ma15062129.
2. L. Weissitsch, F. Staab, K. Durst, A. Bachmaier, Magnetic Materials via High-Pressure Torsion Deformation of Powders, Mater. Trans. advpub (2023). doi:10.2320/matertrans.MT-MF2022026.
3. L. Weissitsch, M. Stückler, S. Wurster, P. Knoll, H. Krenn, R. Pippan, A. Bachmaier, Strain Induced Anisotropic Magnetic Behaviour and Exchange Coupling Effect in Fe-SmCo5 Permanent Magnets Generated by High Pressure Torsion, Crystals. 10 (2020). doi:10.3390/cryst10111026.
4. L. Weissitsch, M. Stueckler, S. Wurster, J. Todt, P. Knoll, H. Krenn, R. Pippan, A. Bachmaier, Manufacturing of Textured Bulk Fe-SmCo5 Magnets by Severe Plastic Deformation, NANOMATERIALS. 12 ARTN 963. doi:10.3390/nano12060963.
5. M. Stückler, C. Teichert, A. Matković, H. Krenn, L. Weissitsch, S. Wurster, R. Pippan, A. Bachmaier, On the magnetic nanostructure of a Co–Cu alloy processed by high-pressure torsion, J. Sci. Adv. Mater. Devices. 6 (2021) 33–41. doi:https://doi.org/10.1016/j.jsamd.2020.09.013.
6. M. Stückler, H. Krenn, R. Pippan, L. Weissitsch, S. Wurster, A. Bachmaier, Magnetic Binary Supersaturated Solid Solutions Processed by Severe Plastic Deformation, Nanomaterials. 9 (2018) 6. doi:10.3390/nano9010006.
7. M. Stückler, L. Weissitsch, S. Wurster, H. Krenn, R. Pippan, A. Bachmaier, Sampling the Cu–Fe–Co phase diagram by severe plastic deformation for enhanced soft magnetic properties, J. Mater. Res. Technol. 12 (2021) 1235–1242. doi:https://doi.org/10.1016/j.jmrt.2021.03.073.
8. A. Inoue, F. Kong, Soft Magnetic Materials, in: A.-G.B.T.-E. of S.M. Olabi (Ed.), Elsevier, Oxford, 2022: pp. 10–23. doi:https://doi.org/10.1016/B978-0-12-803581-8.11725-4.
9. E. Hellstern, L. Schultz, Glass formation in mechanically alloyed transition metal - titanium alloys, Mater. Sci. Eng. 93 (1987) 213–216. doi:https://doi.org/10.1016/0025-5416(87)90426-5.
10. E. Hellstern, L. Schultz, Glass formation in mechanically alloyed transition-metal-Zr alloys, Philos. Mag. B. 56 (1987) 443–448. doi:10.1080/13642818708221330.

11. E. Hellstern, L. Schultz, J. Eckert, Glass-forming ranges of mechanically alloyed powders, J. Less Common Met. 140 (1988) 93–98. doi:https://doi.org/10.1016/0022-5088(88)90371-2.
12. M. Sherif El-Eskandarany, K. Akoi, K. Sumiyama, K. Suzuki, Cyclic crystalline–amorphous transformations of mechanically alloyed Co75Ti25, Appl. Phys. Lett. 70 (1997) 1679–1681. doi:10.1063/1.118667.
13. B.P. Dolgin, M.A. Vanek, T. McGory, D.J. Ham, Mechanical alloying of Ni, CO, and Fe with Ti. Formation of an amorphous phase, J. Non. Cryst. Solids. 87 (1986) 281–289. doi:https://doi.org/10.1016/S0022-3093(86)80002-3.
14. Y.F. Sun, H. Fujii, T. Nakamura, N. Tsuji, D. Todaka, M. Umemoto, Critical strain for mechanical alloying of Cu–Ag, Cu–Ni and Cu–Zr by high-pressure torsion, Scr. Mater. 65 (2011) 489–492. doi:10.1016/J.SCRIPTAMAT.2011.06.005.
15. K. Yamada, T. Maruyama, H. Tanaka, H. Kaneko, I. Kagaya, S. Ito, A thin film head for high density magnetic recording using CoZr amorphous films, J. Appl. Phys. 55 (1984) 2235–2237. doi:10.1063/1.333621.
16. Y. Shimada, H. Kojima, Sputtering of amorphous Co-Zr and Co-Hf films with soft magnetic properties, J. Appl. Phys. 53 (1982) 3156–3160. doi:10.1063/1.331013.
17. M. Naoe, N. Terada, Y. Hoshi, S. Yamanaka, Deposition of amorphous Co-Ta and Co-Zr thin films by means of double ion beam sputtering, IEEE Trans. Magn. 20 (1984) 1311–1313. doi:10.1109/TMAG.1984.1063438.
18. E. Hellstern, L. Schultz, Amorphization of transition metal Zr alloys by mechanical alloying, Appl. Phys. Lett. 48 (1986) 124–126. doi:10.1063/1.96971.
19. G. V Ivanova, N.N. Shchegoleva, The microstructure of a magnetically hard Zr2Co11 alloy, Phys. Met. Metallogr. 107 (2009) 270–275. doi:10.1134/S0031918X09030089.
20. H. Okamoto, Co-Zr (Cobalt-Zirconium), J. Phase Equilibria Diffus. 32 (2011) 169–170. doi:10.1007/s11669-010-9838-x.
21. Y. Aoki, T. Nakamichi, M. Yamamoto, Paramagnetic Behavior in the Non-Stoichiometric Composition of the Laves Phase Compound in the Zr—Co Alloy System, Phys. Status Solidi. 53 (1972) K137–K139. doi:10.1002/pssb.2220530253.
22. H. Fujii, F. Pourarian, W.E. Wallace, Appearance of spontaneous ferromagnetism in non-stoichiometric ZrCo2, J. Magn. Magn. Mater. 24 (1981) 93–96. doi:https://doi.org/10.1016/0304-8853(81)90105-0.
23. A. Hohenwarter, Microstructure, strength and fracture toughness of CuNb nanocomposites processed with high pressure torsion using multi-sector disks, Scr. Mater. 189 (2020) 48–52. doi:https://doi.org/10.1016/j.scriptamat.2020.07.061.
24. A. Tago, C. Nishimura, K. Yanagisawa, Magnetic properties of ion beam sputtered Co-Zr and Co-Zr-Re amorphous films, IEEE Trans. Magn. 21 (1985) 2032–2034. doi:10.1109/TMAG.1985.1064023.
25. A.P. Malozemoff, A.R. Williams, K. Terakura, V.L. Moruzzi, K. Fukamichi, Magnetism of amorphous metal-metal alloys, J. Magn. Magn. Mater. 35 (1983) 192–198. doi:https://doi.org/10.1016/0304-8853(83)90492-4.
26. B. Hofmann, T. Reininger, H. Kronmüller, Influence of the Microstructure on the Magnetization Processes in Nanocrystalline Fe73.5Cu1Nb3Si13.5B9, Phys. Status Solidi. 134 (1992) 247–261. doi:https://doi.org/10.1002/pssa.2211340122.
27. J. Todt, J. Keckes, G. Winter, P. Staron, A. Hohenwarter, Gradient residual strain and stress distributions in a high pressure torsion deformed iron disk revealed by high energy X-ray diffraction, Scr. Mater. 146 (2018) 178–181. doi:https://doi.org/10.1016/j.scriptamat.2017.11.037.
28. T.D. Shen, R.B. Schwarz, J.D. Thompson, Soft magnetism in mechanically alloyed nanocrystalline materials, Phys. Rev. B. 72 (2005) 14431. doi:10.1103/PhysRevB.72.014431.
29. J.M.D. Coey, Magnetism and Magnetic Materials, Cambridge University Press, Cambridge, 2010. doi:DOI: 10.1017/CBO9780511845000.
30. C. Gammer, C. Mangler, C. Rentenberger, H.P. Karnthaler, Quantitative local profile analysis of nanomaterials by electron diffraction, Scr. Mater. 63 (2010) 312–315. doi:https://doi.org/10.1016/j.scriptamat.2010.04.019.
31. K.H.J. Buschow, Crystallization of amorphous Zr1−xCox alloys, J. Less Common Met. 85 (1982) 221–231. doi:https://doi.org/10.1016/0022-5088(82)90073-X.
32. G.F. Zhou, H. Bakker, Magnetic properties of B2-structure CoZr upon ball milling, Phys. B Condens. Matter. 211 (1995) 134–138. doi:https://doi.org/10.1016/0921-4526(94)00965-X.
33. Y. Aoki, T. Nakamichi, M. Yamamoto, Paramagnetic Behavior in the Non-Stoichiometric Composition of the Laves Phase Compound in the Zr—Co Alloy System, Phys. Status Solidi. 53 (1972) K137–K139. doi:https://doi.org/10.1002/pssb.2220530253.
34. M. Woińska, A. Majhofer, J. Gosk, J. Szczytko, Monte Carlo simulations of ferromagnetic nanocomposites, Acta Phys. Pol. A. 122 (2012) 1019–1021. doi:10.12693/APhysPolA.122.1019.
35. M.F. Hansen, S. Mørup, Estimation of blocking temperatures from ZFC/FC curves, J. Magn. Magn. Mater. 203 (1999) 214–216. doi:https://doi.org/10.1016/S0304-8853(99)00238-3.

36. J. Cui, M. Kramer, L. Zhou, F. Liu, A. Gabay, G. Hadjipanayis, B. Balasubramanian, D. Sellmyer, Current progress and future challenges in rare-earth-free permanent magnets, Acta Mater. 158 (2018) 118–137. doi:https://doi.org/10.1016/j.actamat.2018.07.049.
37. B. Balasubramanian, M. Sakurai, C.-Z. Wang, X. Xu, K.-M. Ho, J.R. Chelikowsky, D.J. Sellmyer, Synergistic computational and experimental discovery of novel magnetic materials, Mol. Syst. Des. Eng. 5 (2020) 1098–1117. doi:10.1039/D0ME00050G.